Letter

Underwater Data-Driven Positioning Estimation Using Local Spatiotemporal Nonlinear Correlation

Chengming Luo, Luxue Wang, Xudong Yang, Gaifang Xin, and Biao Wang

Dear Editor,

A global and local canonical correlation analysis (GLCCA) based on data-driven is presented for underwater positioning. Underwater positioning technology can help the underwater targets move predetermined destinations for specific tasks [1]. Since using different sensor, underwater positioning can be divided into three types: inertial navigation, hydroacoustic positioning and geophysical navigation. Underwater inertial navigation method based on the carried sensors has short-term high accuracy, but it is prone to accumulative errors over time and requires external correction [2]. Within the range of pre-deployed hydroacoustic arrays, hydroacoustic positioning method calculates the signal extracted from nodes, but may have fluctuating errors due to the complex hydroacoustic channels [3]. Geophysical positioning method mainly compares the collected information such as seabed terrain, underwater image, or gravity field with the prior knowledge in the reference database [4]. Different positioning methods have their unique merits as well as inherent drawbacks for different applications. How to combine multiple methods to enhance positioning performance has become the holy grail in the field of underwater positioning.

Hydroacoustic positioning has become a widely used technology by solving the signal propagation time or phase from the hydroacoustic array to each mobile transponder [5]. Taking the acoustic signals and array coordinates as inputs, the positioning problem can be transformed into the problem of minimizing the sum of all measurement errors [6]. However, the noisy underwater acoustic signals will make the positioning result have fluctuations [7]. The classical signal to location mapping has the problem that the positioning accuracy is too sensitive to various uncertain noises. Other useful information including network topology can be deeply excavated to reduce the impact of ranging noise on the positioning accuracy. Since the geometric distance of mobile transponder relative to the hydroacoustic array remains unchanged, each mobile transponder will periodically receive the similar acoustic signals caused by the network topology similarity [8]. The classical signal to location mapping can be extended to the topology to signal to location mapping.

Related work: The problem of hydroacoustic positioning based on topology to signal to location mapping can be summarized as establishing a mapping from signal space to location space, including the priori training and positioning testing phases. For a variety of cyber-physical systems, high-quality training datasets were the basis for high performance [9]. To adaptively track multiple surface targets, the acoustic data association strategy integrated with particle filter was applicable to estimate the position and velocity [10]. A canonical correlation analysis (CCA) method was used to discover internal regularities between similar input datasets [11]. However, the nonlinear characteristics of underwater acoustic signals caused by various noises will inevitably weaken the CCA effect. Kernel canonical correlation analysis (KCCA) could handle data nonlinear problems, but did not consider the locality association between underwater acoustic data [12]. Some scholars proposed the local preserving CCA (LPCCA) method to introduce the locality information of associated data [13]. The existing research does not deeply discuss the global and local joint correlation between similar datasets.

These motivate us to propose the GLCCA algorithm from the data-driven perspective. The detail positioning steps are as follows. Drawing on the idea of geophysical navigation, hydroacoustic positioning firstly establishes the priori training sets received from the hydroacoustic arrays communicating with the mobile hydrophone at different locations. The locations of mobile transponder during the priori training phase can usually be obtained from the inertial units. Secondly, the correlation between the received hydroacoustic signals in positioning testing phase and the stored hydroacoustic signals in the priori training phase is analyzed that contains the global and local correlation properties. Thirdly, the locations of mobile hydrophone corresponding to the maximum correlation coefficient is selected as the final positioning output, which can weaken the impact of various uncertain noises on positioning accuracy. The proposed GLCCA algorithm is evaluated and compared with the related CCA, KCCA and LPCCA positioning algorithms.

Problem statement: The overall framework of proposed GLCCA is as shown in Fig. 1. In the underwater area of interest, several hydroacoustic arrays are regularly deployed in advance, while mobile hydrophones and inertial units are installed on the underwater targets [14]. There are n hydroacoustic arrays, whose three-dimensional coordinates are calibrated as $\mathbf{a}=[\mathbf{a}_1,\mathbf{a}_2,\ldots,\mathbf{a}_n]^T$, $\mathbf{a}_i=[x_i,y_i,z_i]^T$. There are m mobile transponders $\mathbf{m}=[\mathbf{m}_1,\mathbf{m}_2,\ldots,\mathbf{m}_m]^T$, $\mathbf{m}_j=[x_j, y_j,z_j]^T$, which can receive the time of arrival (TOA) signal. When establishing prior training database, the received TOA acoustic signals $\mathbf{u}=\left[\mathbf{u}_1,\mathbf{u}_2,\ldots,\mathbf{u}_p\right]\in\mathbb{R}^{n\times p}$ of mobile transponder at different locations $\mathbf{v}^o=[\mathbf{v}_1^o,\mathbf{v}_2^o,\ldots,\mathbf{v}_p^o]\in\mathbb{R}^{q\times p}$ need to be stored, where the parameter p indicates the number of mobile transponders, and the parameter q indicates the coordinate dimension. Considering that there are location errors of mobile hydrophone by the inertial unit during the training phase, the locations can be modelled as $\mathbf{v}=\mathbf{v}^o+\Delta\mathbf{v}$, and the horizontal and vertical spacing between each points is marked as d_H.

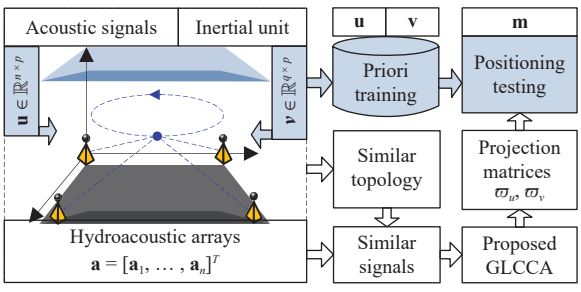

Fig. 1. Overall framework of proposed GLCCA algorithm.

The TOA ranging error is related to the slant range, modelled as $D\times U(e-\varepsilon,e+\varepsilon)$, where D is the slant range; obeys a uniform distribution; $U(\cdot)$ is the error of slant range; ε is the regulator. The correla-

Corresponding author: Chengming Luo.

Citation: C. M. Luo, L. X. Wang, X. D. Yang, G. F. Xin, and B. Wang, "Underwater data-driven positioning estimation using local spatiotemporal nonlinear correlation," *IEEE/CAA J. Autom. Sinica*, vol. 10, no. 8, pp. 1775–1777, Aug. 2023.

C. M. Luo and B. Wang are with Ocean College, Jiangsu University of Science and Technology, Zhenjiang 212100, China (e-mail: chengmingluo@yahoo.com; wangbiao@just.edu.cn).

L. X. Wang and X. D. Yang are with Automation College, Jiangsu University of Science and Technology, Zhenjiang 212100, China (e-mail: 1124606881@qq.com; yangxudong19970731@163.com).

G. F. Xin is with Department of Intelligent Equipment, Changzhou College of Information Technology, Changzhou 213164, and also with the College of Internet of Things Engineering, Hohai University, Changzhou 213022, China (e-mail: xingaifang@ccit.js.cn).

Color versions of one or more of the figures in this paper are available online at http://ieeexplore.ieee.org.

Digital Object Identifier 10.1109/JAS.2023.123288

tion between paired variables $\mathbf{w}_u^T\mathbf{u}$ and $\mathbf{w}_v^T\mathbf{v}$ needs to be reach the maximum value, where the $\mathbf{w}_u \in \mathbb{R}^n$ and $\mathbf{w}_v \in \mathbb{R}^q$ represent two sets of basis vectors. The correlation coefficient of two datasets can be expressed as [15]

$$\rho = \frac{\mathbf{w}_u^T\mathbf{C}_{uv}\mathbf{w}_v}{\sqrt{\mathbf{w}_u^T\mathbf{C}_{uu}\mathbf{w}_u\mathbf{w}_v^T\mathbf{C}_{vv}\mathbf{w}_v}} \tag{1}$$

where $\mathbf{C}_{uu} = \mathbf{u}\mathbf{u}^T \in \mathbb{R}^{n\times n}$ and $\mathbf{C}_{vv} = \mathbf{v}\mathbf{v}^T \in \mathbb{R}^{q\times q}$ represent the within-set covariance matrix; $\mathbf{C}_{uv}$ represents the between-set covariance matrix with $\mathbf{C}_{uv} = \mathbf{C}_{vu}^T$. The solution of optimization problem can be expressed as

$$\begin{cases} \max & \mathbf{w}_u^T\mathbf{C}_{uv}\mathbf{w}_v \\ \text{s.t.} & \mathbf{w}_u^T\mathbf{C}_{uu}\mathbf{w}_u = 1 \\ & \mathbf{w}_v^T\mathbf{C}_{vv}\mathbf{w}_v = 1. \end{cases} \tag{2}$$

The global nonlinear problem is divided into multiple local linear neighborhoods. The similarity matrices $\mathbf{S}_u = \left\{S_{ij}^u\right\}_{i,j=1}^p$ and $\mathbf{S}_v = \left\{S_{ij}^v\right\}_{i,j=1}^p$ containing information about the data local distribution are defined [16]. They can be expressed as

$$S_{ij}^u = \begin{cases} \exp\left(-\left\|\mathbf{u}_i - \mathbf{u}_j\right\|^2/dis_u\right), & i \text{ and } j \text{ are adjacent} \\ 0, & \text{other} \end{cases}$$
$$S_{ij}^v = \begin{cases} \exp\left(-\left\|\mathbf{v}_i - \mathbf{v}_j\right\|^2/dis_v\right), & i \text{ and } j \text{ are adjacent} \\ 0, & \text{other} \end{cases} \tag{3}$$

where $dis_u = \sum_{i=1}^p\sum_{j=1}^p \left\|\mathbf{u}_i - \mathbf{u}_j\right\|^2/\left(p^2-p\right)$ and $dis_v = \sum_{i=1}^p\sum_{j=1}^p \left\|\mathbf{v}_i - \mathbf{v}_j\right\|^2/\left(p^2-p\right)$ represent the average distances of two datasets. The optimization problem considering local characteristics can be formulated as

$$\begin{cases} \max & \mathbf{w}_u^T\mathbf{u}\left(\mathbf{D}_{uv} - \mathbf{S}_u \odot \mathbf{S}_v\right)\mathbf{v}^T\mathbf{w}_v \\ \text{s.t.} & \mathbf{w}_u^T\mathbf{u}\left(\mathbf{D}_{uu} - \mathbf{S}_u \odot \mathbf{S}_u\right)\mathbf{u}^T\mathbf{w}_u = 1 \\ & \mathbf{w}_v^T\mathbf{v}\left(\mathbf{D}_{vv} - \mathbf{S}_v \odot \mathbf{S}_v\right)\mathbf{v}^T\mathbf{w}_v = 1 \end{cases} \tag{4}$$

where, the symbol $\odot$ represents Hadamard product; the expressions $\mathbf{D}_{uu}$, $\mathbf{D}_{uv}$ and $\mathbf{D}_{uu}$ are both symmetric matrices, whose ith diagonal element is equal to the sum ith row elements of the matrices $\mathbf{S}_u \odot \mathbf{S}_u$, $\mathbf{S}_u \odot \mathbf{S}_v$, $\mathbf{S}_v \odot \mathbf{S}_v$, After analyzing the nonlinear data associated with underwater neighborhoods, we introduce the global and local properties into the correlation analysis as follows:

$$\begin{cases} \max & \mathbf{w}_u^T\mathbf{u}\mathbf{G}_{uv}\mathbf{v}^T\mathbf{w}_v \\ \text{s.t.} & \mathbf{w}_u^T\mathbf{u}\mathbf{G}_{uu}\mathbf{u}^T\mathbf{w}_u = 1 \\ & \mathbf{w}_v^T\mathbf{v}\mathbf{G}_{vv}\mathbf{v}^T\mathbf{w}_v = 1 \end{cases} \tag{5}$$

where

$$\mathbf{G}_{uv} = (1-\alpha)\left(\mathbf{D}_{uv} - \mathbf{S}_u \odot \mathbf{S}_v\right) + \alpha\mathbf{C}_{uv}$$
$$\alpha = mean\left(\frac{|\mathbf{D}_{uv} - \mathbf{S}_u \odot \mathbf{S}_v|}{|\mathbf{C}_{uv}|}\right)$$
$$\mathbf{G}_{uu} = (1-\beta)\left(\mathbf{D}_{uu} - \mathbf{S}_u \odot \mathbf{S}_u\right) + \beta\mathbf{C}_{uu}$$
$$\beta = mean\left(\frac{|\mathbf{D}_{uu} - \mathbf{S}_u \odot \mathbf{S}_u|}{|\mathbf{C}_{uu}|}\right)$$
$$\mathbf{G}_{vv} = (1-\gamma)\left(\mathbf{D}_{vv} - \mathbf{S}_v \odot \mathbf{S}_v\right) + \gamma\mathbf{C}_{vv}$$
$$\gamma = mean\left(\frac{|\mathbf{D}_{vv} - \mathbf{S}_v \odot \mathbf{S}_v|}{|\mathbf{C}_{vv}|}\right).$$

The expression $\mathbf{O} = \mathbf{G}_{uu}^{-0.5}\mathbf{G}_{uv}\mathbf{G}_{vv}^{-0.5}$ can be decomposed into $\mathbf{O} = \mathbf{A}\mathbf{E}\{\lambda_k\}_{k\in[1,K]}\mathbf{B}^T$ using singular value decomposition, where $\mathbf{A}$ and $\mathbf{B}$ are the matrices composed of the left and right singular value vectors; $\mathbf{K}$ is the number of eigenvalues; $\mathbf{E}\{\lambda_k\}_{k\in[1,K]}$ is the diagonal matrix composed of singular values greater than 0. The proposed GLCCA algorithm can be further transformed into

$$\begin{cases} \max & \mathbf{A}(:,k)^T\mathbf{O}\mathbf{B}(:,k) \\ \text{s.t.} & \mathbf{A}(:,k)^T\mathbf{B}(:,k) = 1 \\ & \mathbf{A}(:,k)^T\mathbf{B}(:,k) = 1. \end{cases} \tag{6}$$

The updated projection matrices can be expressed as $\boldsymbol{\varpi}_{\boldsymbol{u}} = \mathbf{C}_{uu}^{-0.5}\mathbf{A}$ and $\boldsymbol{\varpi}_{\boldsymbol{v}} = \mathbf{C}_{vv}^{-\mathbf{0.5}}\mathbf{B}$. The set of observations recorded $\{\mathbf{u},\mathbf{v}\}$ in the prior phase into the projection transformations $\{\mathbf{L}_u,\mathbf{L}_v\}$ under $\boldsymbol{\varpi}_{\boldsymbol{u}}$ and $\boldsymbol{\varpi}_{\boldsymbol{v}}$ [13]. The received TOA set $\mathbf{u}_g = \left[u_1^g, u_2^g, \ldots, u_n^g\right]^T$ is converted into the projection transformation $\mathbf{L}_u = \boldsymbol{\varpi}_{\boldsymbol{u}}^T\mathbf{u}_g$ under matrix $\boldsymbol{\varpi}_{\boldsymbol{u}}$. The weighted Euclidean distance d_i^j is calculated between $\mathbf{a}_i$ and $\mathbf{m}_j$, where $d_i^j = \sum_{j=1}^3 \lambda_j(L_{ji}^u - L_j^g)^2$, $i = 1,\ldots,p$, λ_j is the jth eigenvalue; L_{ji}^u is the jth component after the transformation of the ith hydroacoustic array; L_j^g is the jth component. The estimated coordinates $\tilde{\mathbf{m}}_j$ of mobile transponder can be calculated after performing a weighted average of the coordinates of k neighbor points.

Experiments: We use MATLAB R2017b software to verify proposed GLCCA algorithm. The underwater area is set as 600 m × 600 m × 60 m. The UASN is mainly composed of one mobile transponder and four hydroacoustic arrays, marked as $n = 4$. The calibrated coordinates $\mathbf{a}$ of four hydroacoustic arrays are set as [0, 0, −58.5] m, [0, 600, −55.6] m, [600, 0, −56.2] m and [600, 600, −53.4] m considering the ups and downs of water bottom. The acoustic communication radius is set as 1000 m. The ranging error is a random number related to the slant range D. When the ranging error coefficient e is set as {1.25%}, the ranging error distribution intervals are [1.00%,1.50%]D under the regulator ε of {0.25%}. The spacing d_H is set as 5 m, 10 m, 15 m, and 20 m in priori training phase, while the corresponding sampled training points are 14641, 3721, 1681 and 961. 300 samplings M are used to evaluate the positioning accuracy. The parameter q is set as 3. We set the inertial location errors $\Delta\mathbf{v}$ as an increased value over time from 0 to 5.5 m. The proposed GLCCA is compared with CCA [11], KCCA [12], and LPCCA [13] algorithms. We evaluate the positioning performance from the aspects of slant range error, different spacing of prior training, with or without accumulative location errors.

When the spacing d_H is set as 10m, the average errors of CCA, KCCA, LPCCA and GLCCA algorithms are 3.27 m, 2.65 m, 2.54 m and 2.46 m, and the proportion of different algorithms with error less than 4m is 89.67%, 91%, 95.33% and 97.33%, as shown in Fig. 2. Because the CCA algorithm can only deal with linear datasets, the accuracy of positioning performance is poor. Compared with the CCA algorithm, the KCCA algorithm uses the kernel functions to map low-dimensional data for the uniform nonlinear mapping. The LPCCA algorithm considers the local distribution characteristics and achieves the solution of the nonlinear problem by the local linear method. The proposed GLCCA algorithm has high positioning accuracy after considering the global and local correlations. Since the spacing increases from 5 m, 10 m, 15 m to 20 m, the CCA average error increases from 2.42 m, 3.33 m, 4.43 m to 6.02 m, the KCCA average error increases from 1.78 m, 2.70 m, 3.88 m to 5.70 m, the LPCCA average error increases from 1.50 m, 2.67 m, 3.81 m to 5.31 m, while the GLCCA average error increases from 1.47 m, 2.43 m, 3.73 m to 4.80 m, as shown in Fig. 3. As the sampling spacing in the prior training phase increases, the average errors of four algorithms increase as well. The main reason is that the increase of the spacing means that fewer points need to be sampled in the prior training phase, so that the probability of being able to accurately match the exact position in the positioning testing phase becomes lower. No matter how the spacing changes, the positioning accuracy of proposed GLCCA algorithm presents better than other three algorithms.

Fig. 4 shows the different algorithm errors with or without accumulative errors. The inertial location errors $\Delta\mathbf{v}$ are set as an increasement value from 0 to 5.5 m and the spacing d_H is set as 10 m. Compared with Fig. 2, the average positioning errors of CCA, KCCA, LPCCA and GLCCA algorithms increase from 2.46 m, 1.80 m, 1.47 m, 1.42 m to 3.05 m, 2.51 m, 2.32 m, 2.29 m, respectively. Comparing with no accumulative errors of inertial locations, the corresponding maximum positioning errors of CCA, KCCA, LPCCA and GLCCA algorithms are increased from 3.88 m to 5.32 m, 3.80 m to 5.37 m, 2.53 m to 5.10 m, 2.48 m to 5.05 m with accumulative errors of inertial locations. The results indicate that the accumulative errors in the training phase can increase the positioning errors and their divergence trend. Since the accumulative location errors of sampled training points can aggravate the degree of nonlinearity between

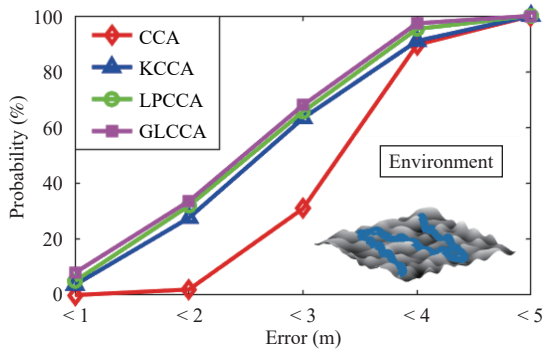

Fig. 2. Positioning error statistics of different algorithm under a blue route.

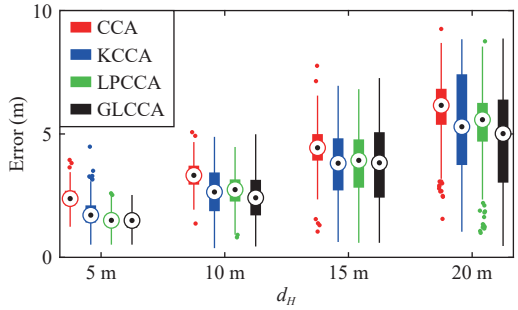

Fig. 3. Positioning error statistics of different algorithms under d_H.

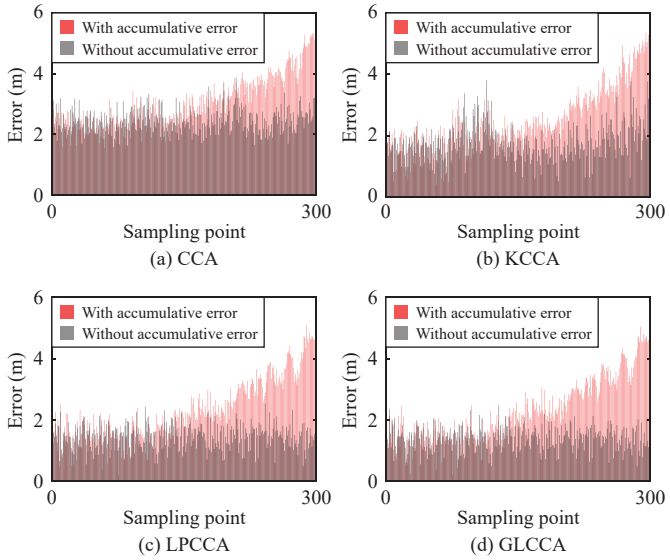

Fig. 4. Different algorithm errors with or without accumulative errors.

datasets, the proposed GLCCA algorithm combines local and global properties to achieve more stable positioning performance.

Conclusions: The proposed GLCCA algorithm analyzes the global and local spatiotemporal nonlinear correlation between two datasets extracted from the prior training and positioning testing phases. The proposed GLCCA introduces the network topology and form an extended topology to signal to location mapping model. Since the spacing increases from 5 m to 20 m, the average errors of CCA, KCCA, LPCCA and GLCCA algorithms are increased from 2.42 m to 6.02 m, 1.78 m to 5.7 m, 1.5 m to 5.31 m, 1.47 m to 4.8 m, respectively. After introducing the accumulative location errors, the average positioning errors of CCA, KCCA, LPCCA and GLCCA algorithms are increased by 0.59 m, 0.71 m, 0.85 m, 0.87 m. The proposed GLCCA algorithm can weaken the sensitivity of uncertain noises on solution process and have a higher positioning accuracy.

Acknowledgments: This work was supported by the National Natural Science Foundation of China (62001195, 52071164), the Basic Science (Natural Science) Research Project of Jiangsu Higher Education Institutions (21KJB460030) and the Applied Basic Research Programs of Changzhou (CJ20220026).

References

[1] J. Yan, Z. W. Guo, X. Yang, X. Y. Luo, and X. Guan, "Finite-time tracking control of autonomous underwater vehicle without velocity measurements," *IEEE Trans. Syst. Man Cybern. Syst*, vol. 52, no. 11, pp. 6759–6773, Nov. 2022.

[2] A. Ramezanifard, M. Hashemi, H. Salarieh, and A. Alasty, "Enhancing the robustness of INS-DVL navigation using rotational model of AUV in the presence of model uncertainty," *IEEE Sensors J*, vol. 22, no. 11, pp. 10931–10939, Jun. 2022.

[3] J. Yan, Y. A. Meng, X. A. Yang, X. Y. Luo, and X. Guan, "Privacy-preserving localization for underwater sensor networks via deep reinforcement learning," *IEEE Trans. Inf. Forensics Security*, vol. 16, pp. 1880–1895, Jan. 2021.

[4] C. C. Tsai and C. H. Lin, "Review and future perspective of geophysical methods applied in nearshore site characterization," *J. Marine Sci. Engn*, vol. 10, no. 3, p. 344, Mar. 2022.

[5] C. M. Luo, B. Wang, Y. X. Cao, G. F. Xin, C. He, and L. Ma, "A hybrid coverage control for enhancing UWSN localizability using IBSO-VFA," *Ad Hoc Netw*, vol. 123, p. 102694, Dec. 2021.

[6] J. Yan, X. Li, X. Yang, X. Y. Luo, C. C. Hua, and X. Guan, "Integrated localization and tracking for AUV with model uncertainties via scalable sampling-based reinforcement learning approach," *IEEE Trans. Syst. Man Cybern. Syst*, vol. 52, no. 11, pp. 6952–6967, Nov. 2022.

[7] H. Y. Zhao, J. Yan, X. Y. Luo, and X. Gua, "Privacy preserving solution for the asynchronous localization of underwater sensor networks," *IEEE/CAA J. Autom. Sinica*, vol. 7, no. 6, pp. 1511–1527, Nov. 2020.

[8] Y. F. Wang, Q. D. Zhou, Z. Y. Xie, and X. J. Lv, "An investigation of acoustic similarity on an underwater structure," *Appl. Mechan. Mat*, vol. 105−107, pp. 84–91, 2012.

[9] J. Zhang, L. Pan, Q. L. Han, C. Chen, S. Wen, and Y. Xiang, "Deep learning based attack detection for cyber-physical system cybersecurity: A survey," *IEEE/CAA J. Autom. Sinica*, vol. 9, no. 3, pp. 377–391, Mar. 2022.

[10] A. Wolek, J. McMahon, B. R. Dzikowicz, and B. H. Houston, "Tracking multiple surface vessels with an autonomous underwater vehicle: Field results," *IEEE J. Ocean. Eng*, vol. 47, no. 1, pp. 32–45, Jan. 2022.

[11] M. S. Ibrahim and N. D. Sidiropoulos, "Blind carbon copy on dirty paper: seamless spectrum underlay via canonical correlation analysis," in *Proc. IEEE Int. Conf. Acoustics, Speech Signal Process*, Toronto, Canada, Apr. 2021, pp. 8123−8127.

[12] J. Manco-Vasquez, S. Van Vaerenbergh, J. Via, and I. Santamaria, "Kernel canonical correlation analysis for robust cooperative spectrum sensing in cognitive radio networks," *Trans. Emerging Telecommun. Technol*, vol. 28, no. 1, p. e2896, Jan. 2017.

[13] J. J. Gu, S. C. Chen, and Y. Zhuang, "Localization in wireless sensor network, using locality preserving canonical correlation analysis," *J. Software*, vol. 21, no. 11, pp. 2883–2891, Nov. 2010.

[14] C. M. Luo, Y. X. Cao, G. F. Xin, B. Wang, and H. L. Wang, "Three-dimensional coverage optimization of underwater nodes under multiconstraints combined with water flow," *IEEE Internet Things J*, vol. 9, no. 3, pp. 2375–2389, Feb. 2022.

[15] D. R. Hardoon, S. Szedmak, and J. Shawe-Taylor, "Canonical correlation analysis: An overview with application to learning methods," *Neural Comput*, vol. 16, no. 12, pp. 2639–2664, Dec. 2004.

[16] X. Z. Gao, Q. S. Sun, H. T. Xu, and Y. M. Li, "2D-LPCCA and 2D-SPCCA: Two new canonical correlation methods for feature extraction, fusion and recognition," *Neurocomputing*, vol. 284, pp. 148–159, Apr. 2018.